CRITICAL ASSESSMENT OF FAILURE CRITERIA FOR ADHESIVELY BONDED COMPOSITE REPAIR DESIGN

Matthew J. Donough[1, 2*], Andrew J. Gunnion[2, 3], Adrian C. Orifici[1], Chun H. Wang[1]
[1] School of Aerospace, Mechanical and Manufacturing Engineering, RMIT University, Australia
[2] Cooperative Research Centre for Advanced Composite Structures, Australia
[3] Advanced Composite Structures Australia Pty Ltd, Australia
*m.donough@student.rmit.edu.au

Keywords: *bonded joints, composites, analytical predictions, finite element analysis*

Abstract

Due to the high stress concentration and non-linear deformation in bonded joints, accurate strength prediction remains challenge. The aim of this paper is to evaluate the accuracies of different failure criteria and computational methodologies for bonded composite joints and their suitability as an engineering design tool. A total of four analytical and four numerical predictive models were evaluated against experimental results obtained from single lap and skin-doubler joints. Experimental observations reveal two main failure modes: cohesive and first-ply fracture. Strain-based models based on cohesive properties were found to be applicable only to joints exhibiting cohesive failure. Fracture mechanics-based models, on the other hand, can predict both cohesive and composite ply failure.

1 Introduction

Adhesive bonded repairs are the preferred method of restoring damaged composite aircraft structure's strength and functionality. With increased confidence and technology maturity, adhesive bonding is now widely accepted for joining and repairing aircraft tertiary and secondary structures. However, certification of bonded repairs of primary structures remains a challenge due to concerns over their long-term durability and lack of non-destructive means of detecting weak interfaces. The challenge is further compounded by the number of potential failure mechanisms in bonded composite joints and the lack of reliable and validated means of predicting the joint strength. ASTM D5573 [1] describes six failure modes in composite joints, based on visual observation of the fracture surfaces, as shown in Fig. 1. In the design and analysis of bonded joints, adhesive failure (or interfacial failure) is usually ignored and is considered as a quality defect. A design analysis of bonded composite repairs needs to consider the potential failure in the adhesive (cohesive) and composite ply (fibre-tear or light fibre-tear), resulting indirectly from high out-of-plane stresses.
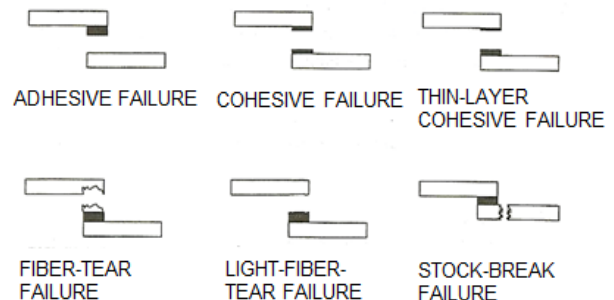

Fig. 1 Failure mechanisms in bonded composite joint

Failure criteria for bonded joint design can be broadly classified as stress/strain based and fracture mechanics based. A wide variety of both analytical and numerical algorithms have been proposed in literature [2-5]. Da Silva et al. [3] compared different analytical methods and used point stress or strain criteria to predict the failure of bonded metallic joints. Castagnetti and Dragoni [4] examined at different modelling techniques which could improve runtime without adversely affecting the stresses within the bondline.

The goal of this paper is to critically review various common analytical and numerical techniques for failure prediction of bonded composite repair. Experimental results are presented for two joint configurations, and the results are compared to failure predictions using various approaches. The focus of the assessment is to consider the predictive capability from the point of view of joint design where failure predictions are required with high confidence and minimal calibration.

2 Experimental

2.1 Manufacturing and test procedure

Experimental studies were carried out to determine the failure loads of two types of bonded composite joints under tensile loading: single-lap joint (SLJ) and skin-doubler joint (SDJ). Table 1 describes the composite layup orientation and adhesive system. The composite adherends were made from Advanced Composite Group's VTM264. The VTM264 is a carbon/epoxy unidirectional tape pre-preg. The composite laminates were cured in accordance with manufacturer's recommendation. Prior to bonding, the bonding surfaces were sanded with 300-grit sandpaper and cleaned. The panels were then secondarily bonded with adhesive, under vacuum at 120°C. The different joint configurations used different epoxy adhesives as shown in Table 1. Any excessive spew, formed during the bonding process, was carefully filed off, to ensure the joint strengths to be conservative. C-scan was performed to inspect for voids within the bondline. Composite tabs, 40 mm long, of the same adherend thickness were bonded onto the composite panels, which were then machined to size as shown in Fig. 2.

Experiments were carried out with an Instron 8510 test machine. Specimens were aligned properly when clamping in the machine grip. Specimens were loaded in tension at a rate of 0.5 mm/min. Specimens sides were painted with a thin layer of white paint to aid visual inspection of crack initiation. Failure is defined as the fracture of the joint or the first significant load drop observed in the experimental load-displacement curve. In the case of the SDJ, the fracture would propagate to the grip area and this had to be machined off to inspect the fracture surfaces.

2.2 Experimental results

Previous research indicates that cohesive failure is more likely to occur when the interfacial plies at the bondline are orientated along the loading direction [6]. In this work, cohesive failure was observed for all SLJ specimens, consistent with the observation reported in [6]. However in the SDJ specimens, the main failure mechanism observed was light-fibre tear or first-ply fracture in the inner adherend as defined by ASTM. Fig. 3 shows the fracture surfaces of the tested specimens.
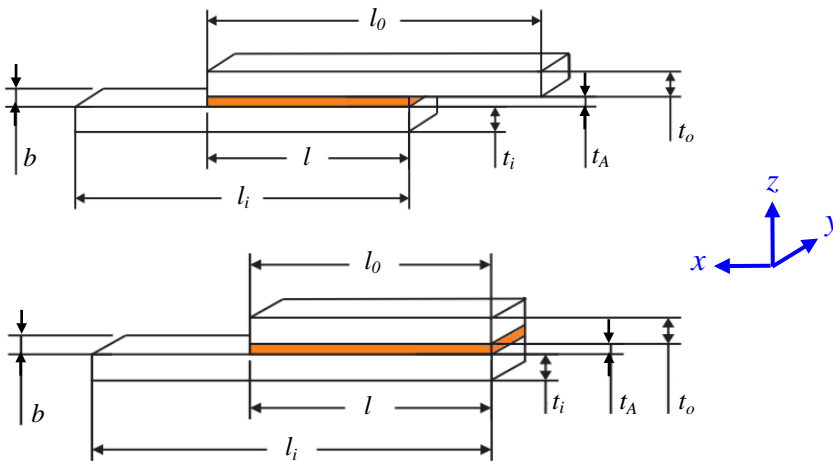
Geometry	SLJ	SDJ
l_0	155	140
l_i	155	280
l	87	140
b	32	20
t_A	0.2	0.2
t_o	4.8	4
t_i	4.8	4
t_{ply}	0.2	0.2

All measurements in mm

Fig. 2 Schematic of the joint specimens; single-lap (top) and skin-doubler (bottom)

Table 1: Specimen details

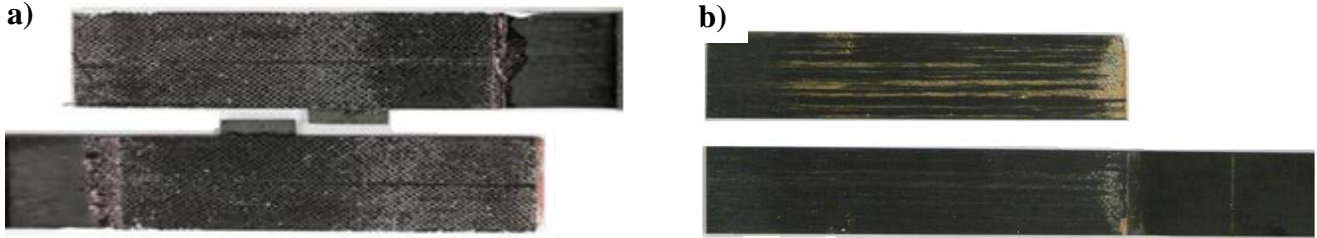| Joint Configuration	Stacking Sequence - inner	Stacking Sequence - outer	Adhesive system	Number of Specimens
Single lap joint	$[0/45/-45/90]_{3S}$	$[0/45/-45/90]_{3S}$	ACG VTA260	3
Skin-doubler joint	$[0_2/45/90/-45]_{2S}$	$[0_2/45/90/-45]_{2S}$	Cytec FM300-2K	4

a)

b)

Fig. 3 Fracture surfaces of tested joints: a) single lap joint specimen and b) skin-doubler specimen

The SLJ failed at a mean tensile load of 1047.2 N/mm with a spread of 7.25%. The SDJ failed at a mean load of 1222 N/mm with a spread of 17.6%. The larger experimental spread was due to the stochastic nature of the damage mechanism. Failure load of the SDJ was taken to be at the onset crack initiation in the joint.

3. Failure Models and Criteria

In this section, the various failure models and criteria applied in this work are reviewed. This includes analytical and numerical approaches using point-based or zone-based stress/strain analysis or those based on fracture mechanics.

3.1 Goland & Reissner

Criteria based on stresses or strains are the traditional methods of assessing material failure. Failure is assumed to occur when the relevant stress or strain attains a critical value at the most highly critical location. The stress distribution within the bondline given by Goland & Reissner is based on a series of shear lag differential equations [7]. The solutions show that the bondline stresses decay to almost zero at some distance away from the overlap termini. When the overlap length is sufficiently large, the maximum shear and peel stresses are independent of the overlap length. The maximum shear and peel stresses for a single-lap joint are expressed as [8]: -

$$\tau_{max} = \frac{\beta \overline{P}}{b} \frac{E_{x,i}' t_i}{E_{x,i}' t_i + E_{x,o}' t_o} \qquad (1)$$

$$\sigma_{max} = k t_o \tau_{max} \qquad (2)$$

where $\beta = \sqrt{\dfrac{G_A}{t_A}\left(\dfrac{1}{E_{x,o} t_o} + \dfrac{1}{E_{x,i} t_i}\right)}$

$k = [E_A/4D_o t_A]^{1/4}$

$D_o = E_{x,o} t_o^2 /12$

$E_x' = E_x/(1-\upsilon_{zx}^2)$

And all other symbols are defined in the Nomenclature section. Using a point stress criterion, maximum joint strength is achieved when either the peak peel or shear stresses exceeded the adhesive fracture stress. Although the model violates the stress free condition at a free edge of continuum mechanics, Goland & Reissner model still forms the basis of latter analytical solutions.

3.2 Hart-Smith

Hart-Smith's joint design methodology assumes maximum joint strength is attained when the adhesive fails in shear. Excessive peel stresses must be reduced through design features so that they do not contribute to failure [9]. The adhesive is modelled as elastic-perfectly plastic. Cohesive failure occurs when the maximum adhesive shear strain is attained. The joint

strength can be predicted with the following equation with the assumption of no thermal mismatch and minimal induced bending [10]: -

$$\overline{P} = \sqrt{2t_A \tau_A \left(\frac{1}{2}\gamma_e + \gamma_p\right) E_{x,i} t_i \left(1 + \frac{E_{x,o} t_o}{E_{x,i} t_i}\right)} \qquad (3)$$

The method is able to predict the strength of joints with a medium-long overlap and a ductile adhesive and is widely employed in the aerospace industry.

3.3   Finite Element Analysis

For joints with complex geometry, a finite element (FE) model is generally required. In the area of FE stress analysis of bonded joints, the pioneering work by Adams and his colleagues have provided insight into behaviour of different joint geometries and non-linear material response [11-14]. FE analysis has the benefit of being able to analyse the through-thickness stresses and individual composite plies. This is especially important for composite joints as failure within the interfacial ply can be determined. In this work, only the gauge section between the grips was modelled. The first five composite plies adjacent to the adhesive bond were modelled individually; the other plies were modelled as an orthotropic laminate. The element aspect ratio was kept below 5. At the termini of the bond region, each element length was 0.05 mm with an aspect ratio of unity. The models were meshed with 2-D plane strain elements. One end of the SLJ and the thicker end of the SDJ was fixed in the x and z translation. The other end was fixed only in the z translation with an applied x direction displacement. Fig. 4 shows the mesh of the FE models and boundary conditions.

Peak stresses occur at the corners of the bi-material interface. The stresses at these points cannot be correlated to the material yield stresses as this will mean that the joint will fail at very low loads. The corner singularity is a complex issue and the actual specimens do not have a mathematically sharp corner. Inevitably there will be a small radius at the corner. The actual corner geometry can be modelled to remove the singularity issue. However this can be difficult to measure and the results will depend on the degree of the fillet. A more common technique is to assess stresses or strains coupled with a characteristic length, l_c [14]. Another consideration is the mesh size sensitivity due to the steep stress gradients at these points. In order to alleviate the mesh sensitivity issue, Tsai et al. [6] and Soutis et al. [15, 16] averaged the stress component over a characteristic length of a ply thickness to predict damage initiation in a double lap joint-repair.

An examination of FE analysis is its ability to correctly predict the failure modes. The composite adherend was assumed to remain elastic. The adhesive was modelled as elastic in one analysis and elastic-perfectly plastic in another analysis. The Hashin quadratic criterion was used to predict composite delamination within the interfacial ply.

$$\sqrt{\left(\frac{\sigma_z^2}{Z_t^2}\right) + \left(\frac{\tau_{zx}^2}{S_{zx}^2}\right)} \geq 1 \qquad (4)$$

The von Mises stress or shear strain, in the middle of the bondline, were evaluated against the adhesive properties. The stresses within the bondline and the interfacial ply were averaged over a characteristic length of 0.2 mm in the x and z direction respectively, from the singularity point.

3.4   Global plastic yielding criterion

In order to overcome problems due to singular stress or strain distribution, Crocombe proposed the global yielding criterion as alternative to predict joint strength [17]. Assuming elastic-perfectly plastic adhesive behaviour, global yielding postulates maximum joint strength is achieved after the adhesive layer has yielded over a specific length l. The simple predictive model of Adams et al. is based on the above hypothesis [18].

$$\tau_{avg} = \frac{\overline{P}}{l} \qquad (5)$$

It is reported that the global yielding criterion can be unconservative for a long bond overlap [3]. A critical damage zone has been suggested as an alternative criterion.
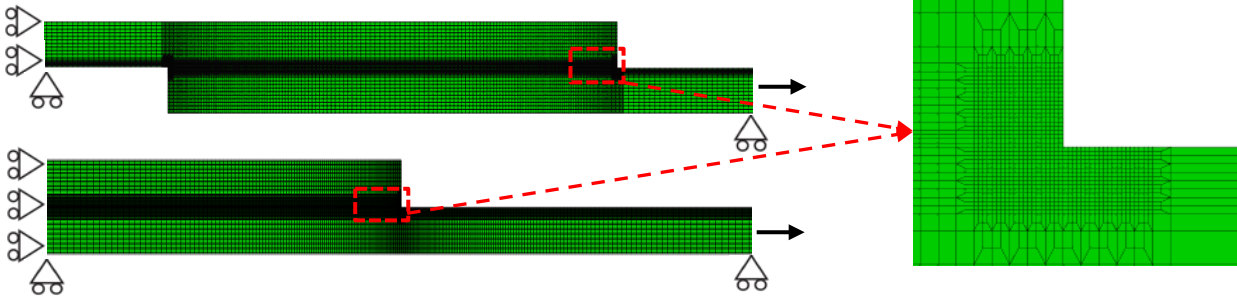
Fig. 4 FE models of single-lap and skin-doubler joints and blown up view of mesh at the corner geometry

Clark & McGregor proposed that cohesive failure could be predicted when the maximum principal stress over a finite length exceeds the adhesive's allowable tensile stress [19]. Sheppard et al. applied the von Mises strain and critical damage area to predict the strength of aluminium and composite joints [20]. To determine the critical zone or length size, model calibration is required based on experimental observations of joints that mimic those in the application of interest.

3.5 Fracture mechanics

The presence of stress singularities has prompted researchers to assume an inherent flaw and use linear elastic fracture mechanics (LEFM) to analyse joints. The strain energy release rate (SERR), G is typically used to characterise crack growth within bonded joints. There are two modes of crack propagation; peeling (mode I) and shearing (mode II). Using the beam theory, the analytical solution for mode I and II SERR within the bondline can be calculated without assuming an initial flaw [21].

$$G_I = \frac{\sigma_{max}^2}{2E_A} t_A \qquad (6)$$

$$G_{II} = \frac{\tau_{max}^2}{2G_A} t_A \qquad (7)$$

The maximum stresses can be derived from Equation 1 and 2. In this work, a single-mode approach was taken where cohesive failure was deemed to have occurred when either G_I or G_{II} exceeded its respective critical value.

3.6 Virtual crack closure technique

Virtual crack closure technique (VCCT) is a numerical approach to fracture mechanics analysis. It assumes the energy required for new crack face creation is equal to that required to close the crack back to its original length [22]. In the linear static analysis with VCCT, a 1.0 mm crack was modelled. The thickness of the blunt crack was 0.01 mm, as shown in Fig. 5. This approach was used by Mall et al. to predict the strength of the skin-doubler joint with varying taper [23]. This was placed either in the middle of the adhesive or ¼ of a ply thickness from the adhesive-composite interface, depending on the fracture mode observed in experiments.
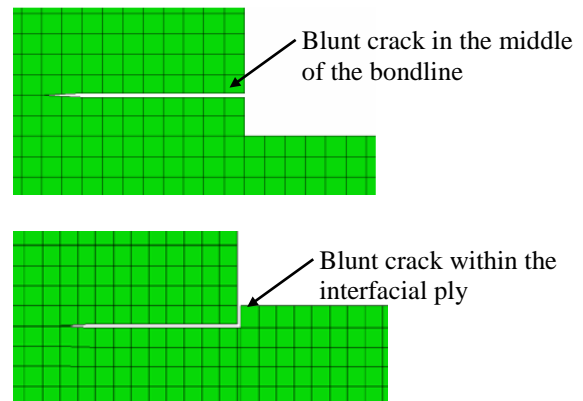

Fig. 5 Position of 1 mm pre-crack in VCCT models

A mixed-mode criterion was used to predict failure. A joint usually fractures in a mixture of mode I and II and the analysis is able predict failure with power law. The linear and quadratic power law criterion, where α equals to 1 and 2 respectively, is suited in capturing mixed mode failure for the general case [24].

$$\left(\frac{G_I}{G_{IC}}\right)^{\alpha} + \left(\frac{G_{II}}{G_{IIC}}\right)^{\alpha} = 1 \qquad (8)$$

3.7 Cohesive zone model

Cohesive zone modelling (CZM) is an advanced numerical analysis technique which models progressive failure of each element. It assumes a process zone ahead of a crack tip in a ductile material. Zero thickness cohesive elements were placed along the crack path observed in the experiments. For the SLJ model, the cohesive elements were placed in the centre of the bondline with adhesive properties. Two cohesive models were created for the SDJ simulation. In the first model, cohesive elements were placed in the middle of the adhesive and at ¼ of ply below the interface, shown in Fig. 6b. A flaw was assumed in the top ply. In the second model, an additional layer of cohesive elements with composite fibre properties was placed between the fibres, shown in Fig 6c.
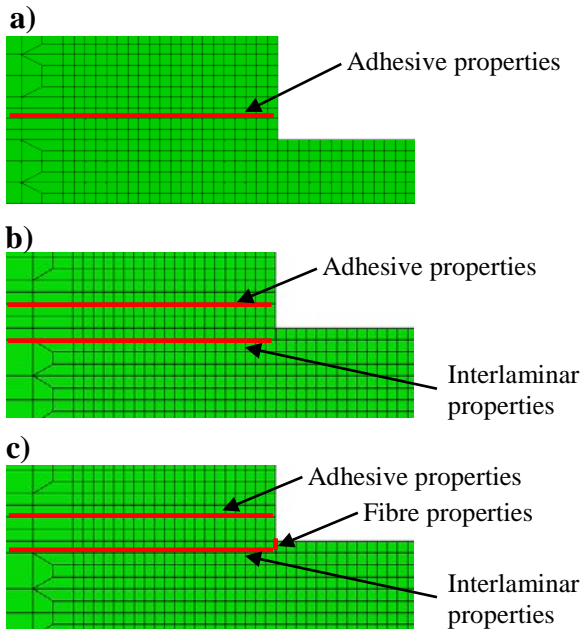
Fig. 6 Placement of zero thickness cohesive elements & properties assigned; a) single-lap joint, b) skin-doubler joint CZM1 and c) skin-doubler joint CZM2

CZM was successfully employed to predict the strength and failure mechanisms of different joint configuration [25, 26]. In the implementation of the CZM applied in this work, the quadratic stress criterion (Eq. 9) and

power law criterion (Eq. 8) were employed to determine onset of damage and ultimate fracture respectively.

$$\left(\frac{\langle t_n \rangle}{t_n^o}\right)^2 + \left(\frac{t_s}{t_s^o}\right)^2 = 1 \qquad (9)$$

The Macaulay operator signifies that a compressive stress does not initiate damage in mode I crack propagation. Different constitutive cohesive behaviour for delamination has been previously studied by Alfano and Crisfield [27]. The bilinear cohesive behaviour was found to be reasonably accurate without being computationally expensive and numerically unstable. Other advanced modelling techniques such as XFEM for analysing bonded joint was considered by Campilho et al. [28] though it was found that the XFEM algorithm is unable to handle crack growth in multi-material interfaces.

4 Determination of Model Parameters

The mechanical properties of the composite and the adhesive used in the analyses are listed in Table 2. The stiffness properties of the adhesives and composite laminate are obtained from the material data sheet from Cytec [29] and Advanced Composite Group [30, 31]. The FM300-2K adhesive shear stress and strain were obtained using the thick adherend single lap joints with the KGR-1 extensometer at room temperature in accordance with ASTM D5656 test standards [29]. The VTA260 adhesive shear stress and strain were determined from short overlap single lap joint at room temperature in accordance with DIN EN2243-1 test standard [30]. The ultimate tensile strength of the adhesives was calculated using the von Mises yield criterion. The double cantilever beam and the end notched flexure specimens were used to determine the mode I and II SERR, respectively, of the adhesive and interlaminar properties of the composite. This was done in accordance with the ASTM D5528 or DIN EN6033 for mode I tests and DIN EN6034 for mode II tests.

Table 2 Material properties for composite unidirectional pre-preg and adhesive systems

VTM264				FM300-2K		VTA260	
Property	*Value*	*Property*	*Value*	*Property*	*Value*	*Property*	*Value*
E_{xx} [MPa]	117000	$G_{I,f}$ [kJ/m^2]	100	E [MPa]	2400	E [MPa]	3000
E_{yy} [MPa]	9510	$G_{II,f}$ [kJ/m^2]	25	G [MPa]	840	G [MPa]	1100
G_{xy} [MPa]	5900	$G_{I,m}$ [kJ/m^2]	0.46	ν	0.4	ν	0.35
G_{yz} [MPa]	3300	$G_{II,m}$ [kJ/m^2]	1.6	X_t [MPa]	94.2	X_t [MPa]	65.8
G_{zx} [MPa]	5900			S_{xy} [MPa]	54.4	S_{xy} [MPa]	38
ν_{xy}	0.32			γ_e	0.055	γ_e	0.035
X_t [MPa]	2459			γ_p	0.580	γ_p	0.190
Z_t [MPa]	48			G_{IC} [kJ/m^2]	1.3	G_{IC} [kJ/m^2]	1.15
S_{xy} [MPa]	88			G_{IIC} [kJ/m^2]	5	G_{IIC} [kJ/m^2]	2.2

The SERR of the FM300-2K were obtained from [10] which used standardised specimens and test method. The interlaminar properties of the VTM264 laminate and VTA260 adhesive were tested in house at RMIT University [32]. The SERR of the fibre properties, $G_{I,f}$ and $G_{II,f}$, cannot be easily measured experimentally with the double cantilever beam or end notched flexure specimens. Therefore it was assumed that the SERR of the fibres to be of a generic carbon fibre value used in analysis found in literature.

5   Comparative Assessment

As an engineering design tool for bonded composite joints, the predictive methodology and its respective failure criteria ideally has to be accurate (within 10% of experimental data), able to predict the failure location, applicable to a generic joint geometry and lastly, easy to use. These predictive failure models will be assessed in terms of the above.

5.1   Accuracy

A well designed and manufactured joint should fail in a cohesive manner [9]. The results obtained from the SLJ experimental results forms an excellent baseline which can be used to assess the accuracy of predictive models. The results from these predictions are presented in Fig. 7.

The linear analytical analysis under-predicted the failure load of the joint with the

point stress criterion. This is expected as structural adhesives will undergo some plastic deformation prior to final fracture. This allows the adhesive to redistribute the load and increase its load carry capability. On the other hand, the global yielding criterion over predicts by a factor of 215%. The joint failed before uniform stress distribution assumed by global yield is achieved. In the case of a long overlap joint, the localized stresses and strains at the termini of the overlap cause failure to occur first.

LEFM prediction with either mode I or II reaches critical level over-predicts by 21% of the experimental failure load. Hart-Smith's failure model was the most accurate of the analytical models for structural adhesives. Despite the presence of peel stress, this indicates that the adhesive fails primarily in shear.
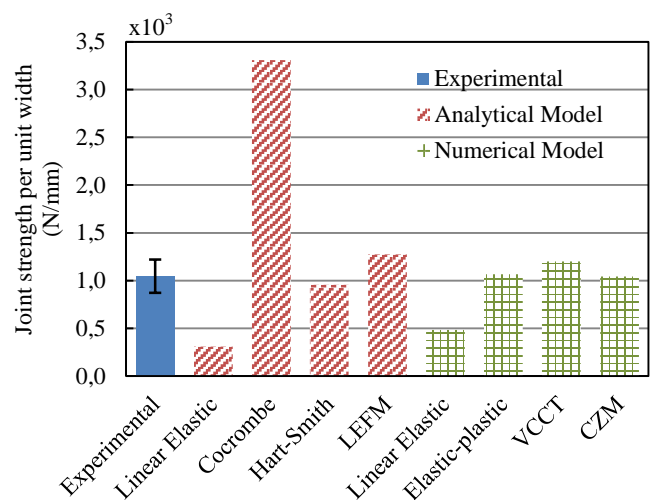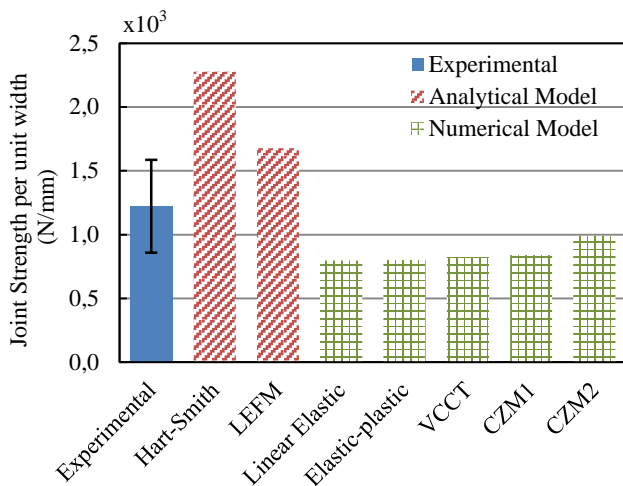

Fig. 7 Single-lap joint static strength predictions

CZM was able to accurately predict the strength of the SLJ specimen. The VCCT provided a similar result to the analytical LEFM solution. The linear numerical prediction with the averaged stress criterion provided with the most conservative result at almost 50% of the experimental failure load. The averaged shear strain criterion in the elastic-plastic analysis was also accurate, slightly over-predicts by 2%.

The SDJ specimens did not fail cohesively, rather by first ply fracture. This implies that the adhesive strength is higher than the composite through-thickness strength. The Hart-Smith and LEFM predictive methods were used in this case as a baseline study to compare the prediction when the wrong failure mode is assumed. The results are presented in Fig. 8. Both analytical solution of Hart-Smith and LEFM over-predicted the failure load of the SDJ due to the disparity between the failure mechanism observed in experiments and the assumed failure mode. The linear numerical analysis showed that composite delamination first initiated at a lower load than those predicted by Hart-Smith and LEFM. The elastic-plastic numerical analysis gives the same prediction as the linear analysis because composite failure was predicted to occur before the adhesive yielded. The VCCT produced similar predicted failure load as the linear elastic FE solution.

CZM1 = cohesive layer in adhesive + interlaminar
CZM2 = cohesive layer in adhesive + interlaminar + fibre

Fig. 8 Skin-doubler joint static strength predictions

In the first cohesive model, it was assumed the main failure modes were the cohesive failure or delamination. A flaw in the fibres of ¼ ply thickness was introduced. The simulated damage initiation load occurred at a load similar to the VCCT simulation. In the second CZM where the fibres are modelled with a layer of cohesive elements, the predicted load was 19% under the experimental failure load. It was still an improvement over the other numerical prediction. The simulation showed that although delamination occurred at a lower load, the fibres were still carrying load. The final fracture of the joint occurred when the fibres finally ruptured.

5.2 Critical failure location

Joint failure models were originally developed for metallic adherends. Therefore the main failure mode is cohesive or interfacial, with the adhesive being the weakest part of the joint. However, as observed in the SDJ experiments, this may not always be the case for bonded composite joints. Failure within the composite is always a possibility even if peel stresses are significantly reduced [26].

The Hashin quadratic criterion for delamination used in the numerical analysis has demonstrated its ability of predicting failure within the interfacial ply. In the analysis of both the SLJ and SDJ, the quadratic criterion was able to correctly indicate if delamination will occur before or after cohesive failure. The stress analysis also showed that the peel stresses in the composite would not exceed an upper threshold level as yielding in the adhesive would redistribute the stresses. Therefore first ply fracture in a SLJ or SDJ can be avoided by ensuring the composite has a through-thickness strength above this level.

With the cohesive model simulation, a small amount of composite delamination occurred first, followed by fibre fracture and then fast crack propagation in the already delaminated layer. However it is difficult to ascertain if this was what happened in the experimental specimens as the fracture occurred very fast. Nevertheless, the model was able to predict failure in the composite ply.

5.3 Computational Efficiency

In terms of practical implementation for engineering design, the global plastic yielding

model is the simplest and only requires two parameters, overlap length and width, in joint design. The influence of the overlap length diminishes after a critical transfer length. Also from the stress analysis of Goland & Reissner, stress uniformity within the bondline is achievable by increasing the adherend tensile modulus and increasing the adherend thickness while minimising the overlap length. Therefore as a result of its simplicity, this methodology is limited to a very specific joint configuration.

The linear-elastic analytical solution and Hart-Smith's elastic-plastic solution are more involved. One can design for the required load carrying capability against the thickness and mechanical properties of adhesive and adherend. However it has been shown that increasing the adhesive thickness will not produce increase in joint strength despite lowering the adhesive stresses. Both models are relatively easy to use and can be solved with a scientific calculator. The point strain criterion used in Hart-Smith's model is more representative of structural adhesives as they undergo some degree of strain after yielding. Both methods can be used to predict joint strength of single lap, double lap and skin-doubler joint with the block end configuration.

FE analysis of bonded joints can be readily done with commercial software and standard modelling techniques. The preparations of the models are more laborious but it can be automated through the use of scripts. Different material response and geometric parameters can be analysed. Depending on the complexity and size of the model, the solving time can range from a few seconds to minutes for a linear or elastic-plastic analysis.

The LEFM analytical approach assumes the joint fail mainly in one of the fracture modes. Mode mixity can be accounted for in the prediction with the Power law. The Power law will have to be solved iteratively. This can be carried out numerically through the use of linear static VCCT analysis. VCCT, however, requires a pre-crack to be modelled. For a well manufactured joint, this may not representative of the joint. For cohesive failure, VCCT with an initial flaw of 1 mm and LEFM produce similar predictions. Therefore LEFM is preferred due the ease of implementation.

The cohesive models are able to simulate damage initiation and propagation. However the model requires prior knowledge of the critical crack path and can be computationally expensive even for a simple model. The solution time can be hours and may be costly for large structures. Also a larger number of material parameters are needed which may require additional characterisation tests if these are not already available for the repair materials under consideration.

6 Conclusion

The predictive models of bonded composite joints must consider both cohesive and composite failure. In the experimental study, the SLJ failed cohesively and the SDJ failed within the composite ply. The main conclusions drawn from the comparative study are as follows: -

1. The model of Hart-Smith gives good prediction for cohesive failure in joints even though it uses a criterion based on only shear strain rather than criteria on shear and peel.
2. The averaged stress/strain criterion gives a conservative prediction and relative robust in predicting the critical failure location (i.e. adhesive or composite).
3. Cohesive zone model gives the most accurate prediction of the failure modes and strength of composite joints. However it requires prior knowledge of the crack path.

Further works on bonded joint strength prediction is to include pre-existing flaws in joints and study how the presence of flaws affects the failure load.

Nomenclature

Symbol	Description
$\overline{P}$	Tensile load per unit width
b	Width
t	Thickness
l	Overlap length
E	Elastic modulus
σ	Direct stress
G	Shear modulus

X, Y, Z	Ultimate direct stresses in x, y, z direction
S	Ultimate shear stress
τ	Shear stress
γ	Shear strain
v	Poisson ratio
t_n, t_s, t_t	Traction stress in mode I, II & III
$t^o_n, t^o_s, t^o_t,$	Maximum traction stresses
G_I	Mode I strain energy release rate
G_{II}	Mode II strain energy release rate

Subscript	Description
A	Adhesive
i	Inner adherend
o	Outer adherend
e	Elastic
p	Plastic
t	Tension
c	Critical allowable

Acknowledgements

References

[1] ASTM D5573-99, *Standard Practice for Classifying Failure Modes in Fiber-Reinforced-Plastic (FRP) Joints*, Annual Book of ASTM Standards, 2005.

[2] L.F.M. da Silva, P.J.C. das Neves, R.D. Adams, J.K. Spelt, Analytical models of adhesively bonded joints--Part I: Literature survey, *International Journal of Adhesion and Adhesives,* Vol. 29, No. 3, pp 319-330, 2009.

[3] L.F.M. da Silva, P.J.C. das Neves, R.D. Adams, A. Wang, J.K. Spelt, Analytical models of adhesively bonded joints--Part II: Comparative study, *International Journal of Adhesion and Adhesives,* Vol. 29, No. 3, pp 331-341, 2009.

[4] D. Castagnetti, E. Dragoni, Standard finite element techniques for efficient stress analysis of adhesive joints, *International Journal of Adhesion and Adhesives,* Vol. 29, No. 2, pp 125-135, 2009.

[5] H. Xiaocong, A review of finite element analysis of adhesively bonded joints, *International Journal of Adhesion and Adhesives,* Vol. 31, No. 4, pp 248-264, 2011.

[6] H.C. Tsai, J. Alper, D. Barrett, Failure Analysis of Composite Bonded Joints, *Proc AIAA Structures, structural dynamics and materials conference and exhibit*, Atlanta, GA, United States, Vol. 41, pp 11, 2000.

[7] M. Goland, E. Reissner, The stresses in cemented joints, *Journal of Applied Mechanics,* Vol. 11, No. 66, pp A17-A27, 1944.

[8] A.A. Baker, R. Jones, F. Rose, *Advances in the bonded composite repair of metallic aircraft structure*, 1st edition., Amsterdam, Elsevier, 2002.

[9] L.J. Hart-Smith, *Analysis and design of advanced composite bonded joints* NASA, CR-2218, 1974.

[10] A.A. Baker, D. Kelly, S. Dutton, *Composite materials for aircraft structures*, 2nd edition., Reston VA, AIAA, 2004.

[11] R.D. Adams, J.A. Harris, The influence of local geometry on the strength of adhesive joints, *International Journal of Adhesion and Adhesives,* Vol. 7, No. 2, pp 69-80, 1987.

[12] J.A. Harris, R.A. Adams, Strength prediction of bonded single lap joints by non-linear finite element methods, *International Journal of Adhesion and Adhesives,* Vol. 4, No. 2, pp 65-78, 1984.

[13] R.D. Adams, N.A. Peppiatt, Stress analysis of adhesive-bonded lap joints, *The Journal of Strain Analysis for Engineering Design,* Vol. 9, No. 3, pp 185-196, 1974.

[14] R.D. Adams, Strength Predictions for Lap Joints, Especially with Composite Adherends. A Review, *The Journal of Adhesion,* Vol. 30, No. 1-4, pp 219-242, 1989.

[15] F.Z. Hu, C. Soutis, Strength prediction of patch-repaired CFRP laminates loaded in compression, *Composites Science and Technology,* Vol. 60, No. 7, pp 1103-1114, 2000.

[16] C. Soutis, D.M. Duan, P. Goutas, Compressive behaviour of CFRP laminates repaired with adhesively bonded external patches, *Composite Structures,* Vol. 45, No. 4, pp 289-301, 1999.

[17] A.D. Crocombe, Global yielding as a failure criterion for bonded joints, *International Journal of Adhesion and Adhesives,* Vol. 9, No. 3, pp 145-153, 1989.

[18] R.D. Adams, J. Comyn, W.C. Wake, *Structural adhesive joints in engineering*, 2nd edition., London, Chapman and Hall, 1997.

[19] J.D. Clark, I.J. McGregor, Ultimate tensile stress over a zone - A new failure criterion for adhesive joints, *J. Adhes.,* Vol. 42, No. 4, pp 227-245, 1993.

[20] A. Sheppard, D. Kelly, L. Tong, A damage zone model for the failure analysis of adhesively bonded joints, *International Journal of Adhesion and Adhesives,* Vol. 18, No. 6, pp 385-400, 1998.

[21] F. Edde, Y. Verreman, On the fracture parameters in a clamped cracked lap shear adhesive joint, *International Journal of Adhesion and Adhesives,* Vol. 12, No. 1, pp 43-48, 1992.

[22] R. Krueger, Virtual crack closure technique: History, approach, and applications, *Applied Mechanics Reviews,* Vol. 57, No. 2, pp 109-143, 2004.

[23] W.S. Johnson, S. Mall, A Fracture Mechanics Approach for Designing Adhesively Bonded Joints, in: W.S. Johnson (Ed.) Delamination and Debonding of Materials, ASTM STP 876, American Society for Testing and Materials, ASTM, Philadelphia, 1985.

[24] G.C. Wassell, J.D. Clark, J.S. Crompton, R.F. Dickson, Fatigue within adhesive bonds, *International Journal of Adhesion and Adhesives,* Vol. 11, No. 2, pp 117-120, 1991.

[25] R.D.S.G. Campilho, M.F.S.F. de Moura, J.J.M.S. Domingues, Using a cohesive damage model to predict the tensile behaviour of CFRP single-strap repairs, *International Journal of Solids and Structures,* Vol. 45, No. 5, pp 1497-1512, 2008.

[26] R.D.S.G. Campilho, M.F.S.F. de Moura, A.M.G. Pinto, J.J.L. Morais, J.J.M.S. Domingues, Modelling the tensile fracture behaviour of CFRP scarf repairs, *Composites Part B: Engineering,* Vol. 40, No. 2, pp 149-157, 2009.

[27] G. Alfano, M.A. Crisfield, Finite element interface models for the delamination analysis of laminated composites: mechanical and computational issues, *International Journal for Numerical Methods in Engineering,* Vol. 50, No. 7, pp 1701-1736, 2001.

[28] R.D.S.G. Campilho, M.D. Banea, A.M.G. Pinto, L.F.M. da Silva, A.M.P. de Jesus, Strength prediction of single- and double-lap joints by standard and extended finite element modelling, *International Journal of Adhesion and Adhesives,* Vol. 31, No. 5, pp 363-372, 2011.

[29] Cyctec Engineering Materials, FM 300-2 film adhesive material description sheet, http://www.cyctec.com, 2007.

[30] Advanced Composite Group, VTA260 flim adhesive material description sheet, http://www.advanced-composites.co.uk, 2011.

[31] Advanced Composite Group, VTM260 series prepreg system material description sheet, http://www.advanced-composites.co.uk, 2009.

[32] J. Ahamed, *Investigation into the tensile fracture mechanism of adhesively bonded composite scarf repairs*, RMIT University, Bachelor Thesis, 2010.

Copyright Statement